Acetyl Cyanide
II. Rotation—Torsion—Vibration Interaction in the Rotational Spectrum

F. Scappini *, H. Mäder, and H. Dreizler

Abteilung für Chemische Physik im Institut für Physikalische Chemie der Universität Kiel, Germany

(Z. Naturforsch. **31 a**, 1398—1407 [1976]; received August 4, 1976)

The rotation—torsion—vibration interaction in acetyl cyanide, CH_3COCN, has been studied in the rotational spectra of the first excited state of the methyl torsion and of the CCN-in-plane bending. A model with two internal degrees of freedom has been used to account for the A—E rotational splittings in the ground state and in the two excited states simultaneously. The constants in the Fourier expansion of the potential hindering the methyl torsion are determined. The results are compared with those obtained in a previous work from the A—E rotational splittings of the ground state only, using a model with one degree of freedom. Group theoretical considerations are made upon the Hamiltonian used in the present analysis.

I. Introduction

The rotation-torsion-vibration (RTV) interaction has been observed in the rotational spectra of two different series of molecules. In the first [1] no direct coupling exists between torsion and vibration in the harmonic force field approximation and the interaction arises from a sum of different contributions: potential torsion-vibration coupling, Coriolis-type coupling, and more complicated RTV couplings. In the second [3—9] there is an additional contribution from the direct coupling of torsional and vibrational angular momenta.

In order to interpret the features of the rotational spectrum in the presence of a RTV interaction one has to extend the simple rigid frame-rigid top (RFRT) model, with only one internal degree of freedom, to a model with more internal degrees of freedom. A complete theoretical treatment including all the vibrations has been given [10—12]. The different approach to the RTV problem contained in the structure relaxation method [13] leads to a Hamiltonian which relates to that derived in Reference [10]. A specific model with only two internal degrees of freedom (from now on it will be simply called RTV model) has been developed in this laboratory [3, 14, 15]. It includes the rotation, torsion and another vibration with which the torsion interacts. No limits are imposed to the amplitude nor to the harmonicity of the vibrational motion considered.

* On leave from Laboratorio di Spettroscopia Molecolare, Bologna, Italy.

Reprint requests to Prof. H. Dreizler, Institut für Physikalische Chemie der Universität Kiel, Abt. Chemische Physik, Olshausenstrasse 40—60, *D-2300 Kiel*, Germany.

Acetyl cyanide belongs to the first series of molecules above mentioned. In Part I [2] results have been reported concerning the analysis of the torsional fine structure in the rotational spectrum of the ground state $(v_a, v_q = 0, 0)$ by the use of a RFRT model. A potential barrier to the methyl torsion of 1207 ± 16 cal/mole has been evaluated from the A—E rotational splittings. With this value it was not possible to fit the rotational spectra of the first excited state of the methyl torsion $(v_a, v_q = 1, 0)$ and of the first excited state of the CCN-in-plane bending $(v_a, v_q = 0, 1)$.

The failure of the RFRT model to interpret simultaneously the rotational spectra in the three states (0, 0) (1, 0), and (0, 1) was the reason why further work on this molecule was undertaken. In the present analysis the RFRT model was extended to a RTV model of the type described in References [14, 15]. Moreover an investigation of the infrared spectra was carried out, since a detailed knowledge of the vibrational spectrum became necessary for the application of the model. This last aspect of the work on acetyl cyanide is treated in Part III [16].

II. Experimental

The experimental details concerning the microwave analysis have been reported in Part I. In the present work only some additional transitions were measured. Table 1 and Table 2 present most of the measured rotational transitions in the (1, 0)- and (0, 1)-states. Figure 1 shows an example of double resonance connections for the (1, 0)-A state, where pumping frequencies are both in the microwave and

Table 1. Observed and calculated rotational transitions in the (1,0)-state. Frequencies are in MHz.

$J_{K-K+}-J'_{K'-K'+}$	Species	$F-F'$	ν_{obs}	$\nu_{unsplit}$ [b]	ν_{calc} [c]
$1_{01}-2_{02}$	A	1−2, 2−3	14138.16	14138.10	14137.97
	E [a]	1−2, 2−3	14144.34	14144.28	
$1_{01}-2_{12}$	A	2−3	19177.18	19177.18	19177.18
	E	2−3	19163.84	19163.84	
$1_{11}-2_{02}$	A	2−3	8105.28	8104.88	8104.81
	E	2−3	8212.74	8212.34	
$2_{02}-2_{11}$	A	1−1, 2−2, 3−3	8461.90	8462.10	8462.19
	E	1−1, 2−2, 3−3	8592.00	8592.20	
$2_{21}-3_{22}$	A	1−2	21428.47	21427.39	21427.51
		2−3	21426.29		
		3−4	21427.73		
	E	—	—		
$2_{12}-3_{13}$	A	1−2, 3−4	19629.49	19629.37	19629.37
	E	1−2, 3−4	19663.43	19663.18	
$2_{02}-3_{03}$	A	1−2, 2−3, 3−4	20854.99	20855.02	20854.87
	E	1−2, 2−3, 3−4	20870.08	20870.11	
$2_{02}-3_{13}$	A	1−2	24668.25	24668.63	24668.57
		2−3, 3−4	24668.67		
	E	1−2	24682.07	24682.46	
		2−3, 3−4	24682.50		
$2_{12}-3_{03}$	A	1−2, 3−4	15816.00	15815.78	15815.67
		2−3	15815.35		
	E	1−2, 3−4	15850.54	15850.36	
$3_{03}-3_{12}$	A	4−4	10647.53	10647.76	10647.71
	E	4−4	10787.96	10788.19	
$3_{21}-3_{30}$	A	2−2, 4−4	32396.76	32397.11	32397.23
		3−3	32398.65		
	E	—	—		
$3_{22}-3_{31}$	A	2−2, 4−4	33104.36	33104.74	33104.95
		3−3	33106.38		
	E	—	—		
$3_{31}-4_{32}$	A	3−4	28830.16	28830.24	28831.59
		4−5	28831.61		
	E	—	—		
$3_{13}-4_{14}$	A	2−3, 3−4, 4−5	26026.48	26026.48	26026.45
	E	2−3, 3−4, 4−5	26049.69	26049.69	
$3_{03}-4_{04}$	A	2−3, 3−4, 4−5	27226.50	27226.51	27226.39
	E	2−3, 3−4, 4−5	27248.19	27248.20	
$3_{03}-4_{14}$	A	2−3, 3−4, 4−5	29840.08	29840.09	29840.15
	E	2−3, 3−4, 4−5	29862.03	29862.04	
$3_{13}-4_{04}$	A	2−3, 3−4, 4−5	23412.92	23412.92	23412.69
	E	2−3, 3−4, 4−5	23435.90	23435.90	
$4_{22}-4_{31}$	A	3−3, 5−5	31500.96	31501.40	31501.80
		4−4	31502.16		
	E	—	—		
$4_{23}-4_{32}$	A	3−3, 5−5	33480.52	33480.97	33481.36
		4−4	33481.88		
	E	—	—		
$4_{14}-5_{15}$	A	3−4, 4−5, 5−6	32328.86	32328.86	32328.89
	E	3−4, 4−5, 5−6	32349.62	32349.62	

Table 1 (continued)

$J_{K-K+}-J'_{K'-K'+}$	Species	$F-F'$	ν_{obs}	$\nu_{unsplit}$ [b]	ν_{calc} [c]
$4_{04}-5_{05}$	A	3−4		33303.89	33303.87
		4−5	33303.89		
		5−6			
	E	3−4		33326.94	
		4−5	33326.94		
		5−6			
$4_{04}-5_{15}$	A	3−4		34942.44	34942.65
		4−5	34942.44		
		5−6			
	E	3−4		34963.42	
		4−5	34963.42		
		5−6			
$4_{14}-5_{05}$	A	3−4		30690.29	30690.10
		4−5	30690.29		
		5−6			
	E	3−4		30713.10	
		4−5	30713.10		
		5−6			

[a] Only E transition checked by MWMWDR and/or by application of frequency sum rules are reported.
[b] Hyperfine center frequency calculated with the constants of Table 3 from Part I.
[c] Rigid rotor frequency calculated with the constants of Table 3 from Part I.

in the radiofrequency regions. The great feasibilities of the double resonance technique, especially in connection with double search experiments, resulted to be a straightforward tool to remove the complication of spectral complexity. It is of significance that we could assign some A-E doublets in the (1, 0)-state, whose components are separated by more than 100 MHz.

III. Rotation—Torsion—Vibration Analysis

a) Hamiltonian

The Hamiltonian is formulated [14, 15] in a rotating coordinate system called Eckart system. By this choice, in this model, no net angular momentum is produced by the vibration and the explicit Coriolis interaction between rotation and vibration is transferred to other terms. The Hamiltonian is restricted to molecules with a plane of symmetry (y, z), in which the vibration considered takes place. There are two starting assumptions in the model theory:

1. the internal rotor has at least a C_3 symmetry about its internal rotation axis and
2. the configuration of the internal rotor is not affected by the vibrations, that is, it is considered to be rigid.

The I^1 representation ($z=a$, $x=c$, $y=b$) is used throughout the derivation:

$$H = H_R + H_T + H_V + H_{RT} + H_{TV} + H_{RV} + H_{RTV} \quad (1)$$

where the subscripts R, T, and V stand for rotation, torsion, and vibration respectively and the subscripts RT, TV, RV, and RTV stand for the corresponding coupled motions. The explicit expressions for the different terms in (1) are:

$$\begin{aligned} H_R + H_{RV} &= A(q) P_z^2 + B(q) P_y^2 + C(q) P_x^2 \\ &\quad + D_{yz}(q)\,(P_y P_z + P_z P_y)\,, \\ H_{RT} + H_{RTV} &= -2\,Q_y(q)\,p_a P_y - 2\,Q_z(q)\,p_a P_z\,, \\ H_T + H_{TV} &= F(q)\,p_a^2 + \tfrac{1}{2} V_3 (1-\cos 3\alpha) \\ &\quad + \tfrac{1}{2} V_6 (1-\cos 6\alpha) \\ &\quad + V'_{3c}\, q\,(1-\cos 3\alpha) \\ &\quad + V''_{3c}\, q^2 (1-\cos 3\alpha)\,, \\ H_V &= \tfrac{1}{4}[M(q)\,p_q^2 + p_q^2\,M(q)] + \tfrac{1}{2} k_{2q}\, q^2 \\ &\quad + \tfrac{1}{2} k_{3q}\, q^3 + \tfrac{1}{2} k_{4q}\, q^4 + W(q) \end{aligned} \quad (2)$$

Footnotes to Table 2:

[a] Only E transitions checked by MWMWDR and/or by application of frequency sum rules are reported.
[b] Hyperfine center frequency calculated with the constants of Table 4 from Part I.
[c] Rigid rotor frequency calculated with the constants of Table 4 from Part I.

Table 2. Observed and calculated rotational transitions in the (0,1)-state. Frequencies are in MHz.

$J_{K-K+}-J'_{K'-K+}$	Species	$F-F'$	ν_{obs}	$\nu_{unsplit}$ [b]	ν_{calc} [c]
$1_{01}-2_{02}$	A	1−2	14208.06	14208.00	14207.91
		2−3			
	E [a]	1−2	14206.93	14206.87	
		2−3			
$1_{01}-2_{12}$	A	2−3	19174.70	19174.77	19174.70
	E	2−3	19173.80	19173.87	
$2_{02}-2_{11}$	A	1−1		8478.59	8478.68
		2−2	8478.49		
		3−3			
	E	1−1		8477.48	
		2−2	8477.38		
		3−3			
$2_{20}-3_{21}$	A	1−2	22151.10	22150.11	22150.16
		2−3	22149.04		
		3−4	22150.49		
	E	—	—		
$2_{12}-3_{13}$	A	1−2	19697.88	19697.78	19697.76
		3−4			
	E	1−2	19696.97	19696.90	
		3−4			
		2−3	19696.68		
$2_{02}-3_{03}$	A	1−2		20940.54	20940.33
		2−3	20940.52		
		3−4			
	E	1−2		20939.11	
		2−3	20939.09		
		3−4			
$2_{12}-3_{03}$	A	1−2	15974.01	15973.92	15973.54
		3−4			
		2−3	15973.56		
	E	1−2	15972.30	15972.16	
		3−4			
		2−3	15971.74		
$2_{02}-3_{13}$	A	2−3	24664.39	24664.31	24664.55
		3−4			
	E	2−3	24663.86	24663.78	
		3−4			
$2_{11}-3_{12}$	A	2−3	23196.86	23197.07	23196.59
		3−4	23197.15		
	E	2−3	23193.76	23194.00	
		3−4	23194.10		
$3_{03}-3_{12}$	A	4−4	10735.20	10735.26	10734.94
	E	4−4	10732.22	10732.28	
$3_{21}-3_{30}$	A	2−2	32179.24	32179.86	32179.85
		4−4			
		3−3	32181.15		
	E	—	—		
$3_{22}-3_{31}$	A	2−2	32926.76	32927.38	32927.29
		4−4			
		3−3	32928.66		
	E	—	—		

$J_{K-K+}-J'_{K'-K+}$	Species	$F-F'$	ν_{obs}	$\nu_{unsplit}$ [b]	ν_{calc} [c]
$3_{13}-3_{22}$	A	2−2	23304.58	23305.28	23304.88
		3−3	23306.23		
		4−4	23304.92		
	E	—	—		
$3_{13}-4_{14}$	A	2−3		26109.85	26109.94
		3−4	26109.85		
		4−5			
	E	2−3		26108.83	
		3−4	26108.83		
		4−5			
$3_{30}-4_{31}$	A	2−3	29079.85	29079.28	29080.23
		4−5			
		3−4	29078.25		
	E	—	—		
$3_{31}-4_{32}$	A	2−3	29002.36	29001.84	29002.78
		4−5			
		3−4	29000.86		
	E	—	—		
$3_{22}-4_{23}$	A	3−4	28604.82	28605.27	28605.45
		4−5	28605.48		
	E	—	—		
$3_{13}-4_{04}$	A	2−3		23588.87	23588.38
		3−4	23588.87		
		4−5			
	E	2−3		23586.70	
		3−4	23586.70		
		4−5			
$3_{03}-4_{14}$	A	2−3		29833.60	29834.16
		3−4	29833.60		
		4−5			
	E	2−3		29833.60	
		3−4	29833.60		
		4−5			
$3_{03}-4_{04}$	A	2−3		27312.68	27312.60
		3−4	27312.67		
		4−5			
	E	2−3		27311.37	
		3−4	27311.36		
		4−5			
$4_{22}-4_{31}$	A	3−3	31239.84	31240.24	31241.15
		5−5			
		4−4	31241.06		
	E	—	—		
$4_{23}-4_{32}$	A	3−3	33323.35	33323.71	33324.62
		5−5			
		4−4	33324.44		
	E	—	—		

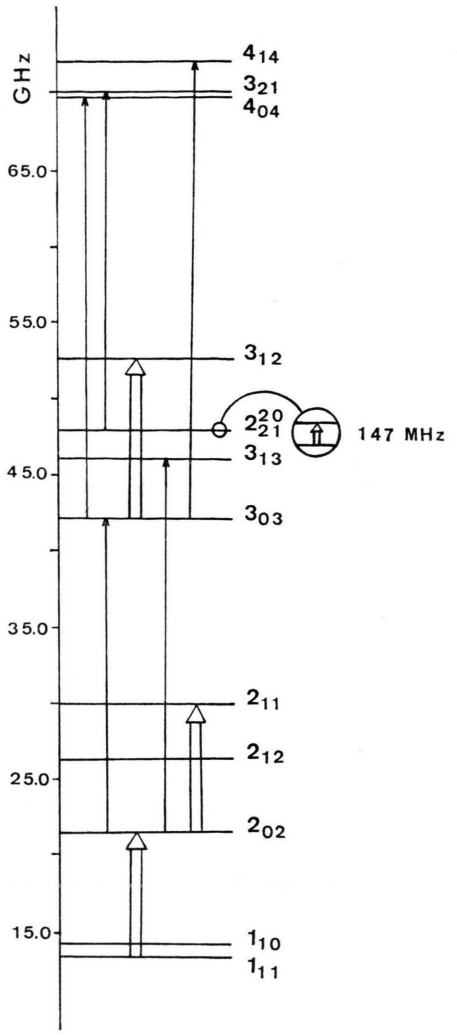

Fig. 1. Example of double resonance connections for CH_3COCN in the (1,0)-A state.

where:

P_g operator of the total angular momentum component with respect to the g-axis of the Eckart system, $g = x, y, z$;

p_α $-i(\partial/\partial\alpha)$, operator of the torsional angular momentum;

p_q $-i(\partial/\partial q)$, operator of the vibrational momentum;

q vibrational coordinate;

α torsional angle;

$$A(q) = (h/8\pi^2)\,(I_{yy} - \lambda_y^2 I_\alpha)/r\Delta\,;$$
$$B(q) = (h/8\pi^2)\,(I_{zz} - \lambda_z^2 I_\alpha)/r\Delta\,;$$
$$C(q) = (h/8\pi^2)/I_{xx}\,;$$
$$D_{yz}(q) = -(h/8\pi^2)\,(I_{yz} - \lambda_y \lambda_z I_\alpha)/r\Delta\,;$$
$$Q_y(q) = (h/8\pi^2)\,(\lambda_y I_{zz} - \lambda_z I_{yz})/r\Delta\,;$$
$$Q_z(q) = (h/8\pi^2)\,(\lambda_z I_{yy} - \lambda_y I_{yz})/r\Delta\,;$$
$$F(q) = (h/8\pi^2)/r I_\alpha\,;$$
$$M(q) = (h/4\pi^2)/G^{-1};$$
$$r(q) = 1 - I_\alpha(\lambda_y^2 I_{zz} - 2\lambda_y \lambda_z I_{yz} + \lambda_z^2 I_{yy})/\Delta\,;$$
$$\Delta(q) = I_{yy} I_{zz} - I_{yz}^2\,;$$

I_{yz} = product of inertia;

$I_{gg}(q)$ moments of inertia about the g-axis of the Eckart system, $g = x, y, z$;

λ_g direction cosine of the internal rotation axis with respect to the g-axis, $g = x, y, z$;

I_α moment of inertia of the top about its symmetry axis;

$$G^{-1}(q) = \sum_k m_k\,(\partial \mathbf{r}_k/\partial q)^2\,,$$

reduced mass for the vibration (m_k mass and $\mathbf{r}_k$ position vector of the atom k).

The term $W(q)$ arises from the translation of the classical Hamiltonian into its quantum mechanical form. The potential energy in (2) is:

$$V(\alpha, q) = \tfrac{1}{2} V_3\,(1 - \cos 3\alpha) + \tfrac{1}{2} V_6\,(1 - \cos 6\alpha) + \tfrac{1}{2} k_{2q}\, q^2 + \tfrac{1}{2} k_{3q}\, q^3 + \tfrac{1}{2} k_{4q}\, q^4 + V'_{3c}\, q\,(1 - \cos 3\alpha) + V''_{3c}\, q^2\,(1 - \cos 3\alpha) \qquad (3)$$

it contains three- and six-fold terms for the pure torsion, V_3 and V_6; harmonic, cubic and quartic force constants for the vibration, k_{2q}, k_{3q}, and k_{4q}; and two potential coupling terms for the torsion-vibration interaction, V'_{3c} and V''_{3c}. The potential coupling terms represent cubic and quartic force constants in the limit of small amplitude torsional motion.

For the numerical treatment of the Hamiltonian the q-dependent kinetic coefficients are expanded in power series of q, truncated after the second order terms:

$$Y = Y^0 + Y'\,q + Y''\,q^2 \qquad (4)$$

where Y stands for A, B, C, D_{yz}, Q_y, Q_z, F, M, and W. The expansion coefficients in (4) are molecular constants depending on atomic masses, molecular structure and vibrational mode.

The Hamiltonian (1) consists of three limiting parts:

$$H_R^0 = A^0 P_z^2 + B^0 P_y^2 + C^0 P_x^2\,,$$
$$H_T^0 = F^0 p_\alpha^2 + \tfrac{1}{2} V_3\,(1 - \cos 3\alpha) + \tfrac{1}{2} V_6\,(1 - \cos 6\alpha)\,,$$
$$H_V^0 = \tfrac{1}{2} M^0 p_q^2 + \tfrac{1}{2} k_{2q}\, q^2\,, \qquad (5)$$

all the other terms which enter in (1) account for the interactions occurring by the coupling of the three motions. The limiting parts (5) and the Hamiltonian (1) can be classified according to the symmetry groups defined in Table 3. The correlations among the symmetry species are given in Table 4. Since the selection rules specified under the groups C_{3v} and D_3 result in:

$$A_1 \longleftrightarrow A_2 \quad \text{and} \quad E \longleftrightarrow E$$

we will omit in the following the subscripts from A_1 and A_2.

Table 3. Elements of the invariance groups of Hamiltonian (1) and its limiting parts (5). The group elements are defined by the given operations on the coordinates. I^1 representation.

$V(H_R{}^0)$
E : $\Phi \to \Phi,\ \Theta \to \Theta,\ \chi \to \chi$
C_{2x}: $\Phi \to \Phi+\pi,\ \Theta \to \pi-\Theta,\ \chi \to -\chi$
C_{2y}: $\Phi \to \Phi+\pi,\ \Theta \to \pi-\Theta,\ \chi \to \pi-\chi$
C_{2z}: $\Phi \to \Phi,\ \Theta \to \Theta,\ \chi \to \chi+\pi$

$C_{3v}(H_T{}^0)$
E : $\alpha \to \alpha$
C_3 : $\alpha \to \alpha+2\pi/3$
σ_v : $\alpha \to -\alpha$

$C_s(H_V{}^0)$ [a]
E : $q \to q$
σ_h : $q \to -q$

$D_3(H)$
E : $\Phi \to \Phi,\ \Theta \to \Theta,\ \chi \to \chi,\ \alpha \to \alpha,\ q \to q$
C_3 : $\Phi \to \Phi,\ \Theta \to \Theta,\ \chi \to \chi,\ \alpha \to \alpha+2\pi/3,\ q \to q$
C_{2x}: $\Phi \to \Phi+\pi,\ \Theta \to \pi-\Theta,\ \chi \to -\chi,\ \alpha \to -\alpha,\ q \to q$

[a] In the present case the symmetry species of the vibrational functions is A′ only, unter C_s.

$D_3(H)$	$V(H_R{}^0)$
A_1	A
	B_x
A_2	B_y
	B_z

$D_3(H)$	$C_{3v}(H_T{}^0)$
A_1	A_1
A_2	A_2
E	E

$D_3(H)$	$C_s(H_V{}^0)$
A_1	A′
	A″

Table 4. Correlation of the D_3 and V, C_{3v}, C_s groups respectively. For the definition of the groups see Table 3. The correlation is established by operations on coordinates which are common to both the considered groups.

As described in Ref. [15], H_T of (1) is set up in the basis of free rotor functions

$$U_m = (1/\sqrt{2\pi}) \exp\{i\, m\, \alpha\}, \quad m = 0, \pm 1, \pm 2, \ldots .$$

Diagonalization leads to the energies of the pure torsional levels $E_{v_a\sigma}$ and to the eigenfunctions $U_{v_a\sigma}(\alpha)$. Each v_a level is split into one non-degenerate $A(\sigma = 0)$ and one degenerate $E(\sigma = \pm 1)$ sublevel according to the symmetry species of the C_{3v} group. In the next step the energy matrix of $H_T + H_V + H_{TV}$ is set up in the product basis of the torsional eigenfunctions $U_{v_a\sigma}(\alpha)$ and the harmonic oscillator functions $H_{v_q}(q)$. After diagonalization the eigenvalues $E_{v_a\sigma v_q}$ and the eigenfunctions $\Phi_{v_a\sigma v_q}(\alpha, q)$ become available. Each torsion-vibration level is still split into A- and E-sublevels according to the symmetry species of a subgroup of the $C_{3v} \otimes C_s$ product group. In the final step of setting up the matrix of the total Hamiltonian (1) the basis functions are taken to be the products of the torsion-vibration eigenfunctions $\Phi_{v_a\sigma v_q}(\alpha, q)$ and the symmetric rotor functions $\Psi^x_{JKM}(\Phi, \chi, \Theta)$, where Φ, χ, Θ, are the Eulerian angles. The following diagonalization yields, for each (v_a, v_q)-state, the rotational spectrum, which is split into A and E components, according to the symmetry species of the D_3 inner group.

In order to evaluate the kinetic coefficients in (4) the r_0-structure from Ref. [17] is taken in place of the r_e-structure, which should be known for the analysis. The mode of the vibration considered was given by the normal coordinate analysis performed in a harmonic oscillator approximation [16]. From these calculations the CCN-in-plane bending appeared to be mainly a mixture of CCN- and CCC-angle deformations in the ratio 10 : 1 and with the same phase, see Figure 2. The vibrational coordinate q was chosen to be the deviation of the CCN-angle from equilibrium (180°) and it is defined to be positive for a displacement of the N atom toward the methyl group. With the above assumptions the components of the moment of inertia tensor, Eq. (17) of Ref. [15], and the kinetic coefficients of Hamiltonian (1) were calculated for 11 values of q, varying from $-12°$ to $+12°$, and fitted to a fifth order polynomial. In fact an estimate of the mean amplitude of the CCN-in-plane bending by:

$$\sqrt{\langle v_q | q^2 | v_q \rangle} = \sqrt{3\, M^0/2\, \omega},$$

where ω is the vibrational frequency corresponding to $v_a, v_q = 0, 0 \to 0, 1$ for $v_q = 1$ gives approxi-

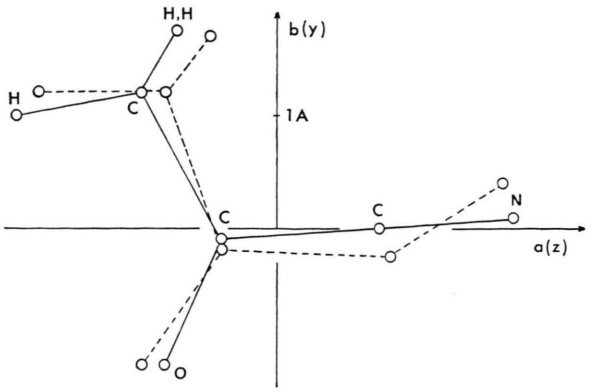

Fig. 2. CCN-in-plane bending mode for CH_3COCN.

mately 12°. The expansion coefficients up to the second order, for the calculated vibrational mode, are given in Table 5.

The numerical treatment of the eigenvalue problem of the Hamiltonian (1) was performed by exact diagonalization of the energy matrices.

b) Results

For the analysis of the spectra the energy level scheme resulting from the eigenvalues of the Hamiltonian (1) have to be compared with the experimental data. In principle all the parameters which enter in the Hamiltonian (1) can be fitted, but, due to the limited number of experimental informations, in the present case only part of the potential constants were fitted. The parameters which enter in the kinetic part were fixed at the values calculated as described above.

Five of the seven potential constants could be determined, that is, V_3, V_6, k_{2q}, V'_{3c}, and V''_{3c}. The last two, k_{3q} and k_{4q}, were set to zero since their determination would involve more infrared data than those presently available, from hot bands and combination band measurements. Within the approximations done the harmonic force constant for the CCN-in-plane bending is given by $k_{2q}=\omega^2/M^0$. The remaining four potential constants were fitted to the A-E splittings of the rotational transitions of the states (0, 0), (0, 1), and (1, 0) simultaneously. In the case of the (1, 0)- and (0, 1)-states only transitions accurately checked by MWMWDR technique and/or by application of frequency sum rules were used in this procedure. The observed and calculated A-E rotational splittings are presented in Table 6. The potential constants which were fitted, together with those assumed and precalculated, are listed in Table 7. For comparison Table 8 shows the results obtained from the ground state A-E rotational splittings by the RFRT model theory [2]. In the latter case the potential function was expressed as one-term cosine function, $(V_3/2)(1-\cos 3\alpha)$. Table 9 presents the correlation coefficients of the four potential constants fitted and Table 10 gives the mean partial derivatives of the A-E rotational splittings with respect to these constants. The vibrational level scheme, calculated with the help of the

Table 5. Components of the generalized tensor of inertia [a] and kinetic coefficients in the Hamiltonian (1). I^1 representation. Conversion factor 505.376 amu·Å²·GHz, atomic masses [20].

I_{zz}^0	amu·Å²	49.203090	I_{zz}'	amu·Å²·rad^{-1}	2.158391	I_{zz}''	amu·Å²·rad^{-2}	3.901488
I_{yy}^0	amu·Å²	121.686773	I_{yy}'	amu·Å²·rad^{-1}	−3.552942	I_{yy}''	amu·Å²·rad^{-2}	−22.728424
I_{xx}^0	amu·Å²	167.691669	I_{xx}'	amu·Å²·rad^{-1}	−1.394551	I_{xx}''	amu·Å²·rad^{-2}	−18.826936
			I_{yz}'	amu·Å²·rad^{-1}	14.147340	I_{yz}''	amu·Å²·rad^{-2}	−1.288640
λ_z^0		0.4852	λ_z'	rad^{-1}	−0.1313	λ_z''	rad^{-2}	−0.0037
λ_y^0		0.8744	λ_y'	rad^{-1}	0.0729	λ_y''	rad^{-2}	−0.0108
$(G^{-1})^0$	amu·Å²·rad^{-2}	6.1346	$(G^{-1})'$	amu·Å²·rad^{-3}	0.2306	$(G^{-1})''$	amu·Å²·rad^{-4}	3.2177
I_α^0	amu·Å²	3.19						
A^0	GHz	10.434177	A'	GHz·rad^{-1}	−0.623286	A''	GHz·rad^{-2}	−0.414851
B^0	GHz	4.239605	B'	GHz·rad^{-1}	0.112100	B''	GHz·rad^{-2}	0.965897
C^0	GHz	3.013722	C'	GHz·rad^{-1}	0.025063	C''	GHz·rad^{-2}	0.338564
D_{yz}^0	GHz	0.118735	D_{yz}'	GHz·rad^{-1}	−1.263347	D_{yz}''	GHz·rad^{-2}	0.158880
Q_z^0	GHz	−5.166662	Q_z'	GHz·rad^{-1}	2.768780	Q_z''	GHz·rad^{-2}	0.112943
Q_y^0	GHz	−3.764696	Q_y'	GHz·rad^{-1}	0.221595	Q_y''	GHz·rad^{-2}	−1.049427
F^0	GHz	163.818	F'	GHz·rad^{-1}	−1.941	F''	GHz·rad^{-2}	1.150
M^0	GHz·rad²	164.762	M'	GHz·rad	−6.193	M''	GHz	−86.153
			W'	GHz·rad^{-1}	6.029993	W''	GHz·rad^{-2}	95.600765

[a] See Eq. (17) of Reference [15].

constants from Tables 5 and 7 is shown in Figure 3. Table 11 summarizes the results obtained from the analyses of molecules presenting a RTV interaction and up to now studied in this laboratory.

Table 6. Observed and calculated A—E rotational splittings, in MHz.

$J_{K-K+}-J'_{K'-K'+}$	v_a, v_Q	$(\nu_E-\nu_A)_{obs}$	$(\nu_E-\nu_A)_{calc}$ [b]	Δ [c]
$1_{11}-2_{12}$	0,0 [a]	0.00	−0.27	0.27
$1_{10}-2_{21}$		−5.76	−5.80	0.04
$1_{01}-2_{12}$		−0.62	−0.70	0.08
$2_{20}-3_{21}$		−4.13	−4.26	0.13
$2_{12}-3_{13}$		−0.43	−0.46	0.03
$2_{02}-3_{13}$		−0.48	−0.52	0.04
$2_{02}-3_{03}$		−0.66	−0.76	0.10
$2_{21}-3_{22}$		1.92	1.88	0.04
$3_{21}-3_{30}$		26.66	26.88	−0.22
$3_{22}-3_{31}$		−32.00	−31.53	0.47
$3_{30}-4_{31}$		−18.67	−18.55	−0.12
$3_{31}-4_{32}$		15.89	15.49	0.40
$3_{12}-4_{13}$		−1.83	−1.93	0.10
$3_{03}-4_{04}$		−0.63	−0.73	0.10
$3_{03}-4_{14}$		0.00	−0.32	0.32
$3_{13}-4_{04}$		−0.82	−0.96	0.14
$4_{22}-4_{31}$		10.17	10.82	−0.65
$4_{23}-4_{32}$		−15.37	−15.22	−0.15
$4_{23}-5_{14}$		−1.66	−2.06	0.40
$1_{01}-2_{02}$	1,0	6.18	5.79	0.39
$1_{01}-2_{12}$		−13.34	−14.35	1.01
$1_{11}-2_{02}$		107.46	106.30	1.16
$2_{02}-2_{11}$		130.10	129.23	0.87
$2_{12}-3_{13}$		33.81	33.48	0.33
$2_{02}-3_{03}$		15.09	15.02	0.07
$2_{02}-3_{13}$		13.83	13.35	0.48
$2_{12}-3_{03}$		34.58	35.16	−0.58
$3_{03}-3_{12}$		140.43	141.93	−1.50
$3_{13}-4_{14}$		23.21	23.33	−0.12
$3_{03}-4_{04}$		21.69	22.00	−0.31
$3_{03}-4_{14}$		21.95	21.66	0.29
$3_{13}-4_{04}$		22.98	23.67	−0.69
$4_{14}-5_{15}$		20.76	21.08	−0.32
$4_{04}-5_{05}$		23.05	23.55	−0.50
$4_{04}-5_{15}$		20.98	20.73	+0.25
$4_{14}-5_{05}$		22.81	23.89	−1.08
$1_{01}-2_{02}$	0,1	−1.13	−1.02	−0.11
$1_{01}-2_{12}$		−0.90	−0.92	0.02
$2_{02}-2_{11}$		−1.11	−1.41	0.30
$2_{12}-3_{13}$		−0.88	−0.73	−0.15
$2_{02}-3_{03}$		−1.43	−1.19	−0.24
$2_{12}-3_{03}$		−1.76	−1.29	−0.47
$2_{02}-3_{13}$		−0.53	−0.63	0.10
$2_{11}-3_{12}$		−3.07	−2.48	−0.59
$3_{03}-3_{12}$		−2.98	−2.70	−0.28
$3_{13}-4_{14}$		−1.02	−0.88	−0.14
$3_{13}-4_{04}$		−2.17	−1.70	−0.47
$3_{03}-4_{14}$		0.00	−0.31	0.31
$3_{03}-4_{04}$		−1.31	−1.11	−0.20

[a] The observed A—E rotational splittings for the ground state are taken from Table 1 of Part I.
[b] Calculated with the Hamiltonian (1) and the constants from Table 5 and 7.
[c] $\Delta=(\nu_E-\nu_A)_{obs}-(\nu_E-\nu_A)_{calc}$.

Table 7. Potential constants in the Hamiltonian (1) determined by a least squares fit to the A—E rotational splittings of the (0,0)-, (1,0)-, and (0,1)-states from Table 6. Quoted standard errors.

V_3	GHz	12346 ± 14
	cal·mole^{-1}	1177 ± 2
V_6	GHz	−142 ± 11
	cal·mole^{-1}	−13 ± 2
V_{3c}'	GHz·rad^{-1}	2649 ± 255
	cal·mole^{-1}·rad^{-1}	254 ± 24
V_{3c}''	GHz·rad^{-2}	5952 ± 390
	cal·mole^{-1}·rad^{-2}	568 ± 37
k_{2Q} [a]	GHz·rad^{-2}	168948
	cal·mole^{-1}·rad^{-2}	16113
k_{3Q} [b]	GHz·rad^{-3}	0
k_{4Q} [b]	GHz·rad^{-4}	0

[a] $k_{2Q}=\omega^2/M^0$, $\omega=5276$ GHz (176 cm^{-1}) measured vibrational frequency, M^0 from Table 5. This force constant differs by definition from that used in the normal coordinate analysis [16].
[b] Assumed.

Table 8. Results obtained from the ground state A—E rotational splittings only, by application of the RFRT model [2].

I_a	amu·Å^2	3.14	± 0.04
λ_z		0.5155	± 0.0040
F	GHz	166.97	± 2.02
V_3	GHz	12655	±168
	cal·mole^{-1}	1207	± 16

Table 9. Correlation coefficients of the fitted potential constants V_3, V_6, V_{3c}', V_{3c}''.

V_3	1.000			
V_6	0.046	1.000		
V_{3c}'	0.901	−0.250	1.000	
V_{3c}''	−0.843	−0.351	−0.637	1.000

Table 10. Mean partial derivatives [a] of the A—E rotational splittings (Table 6) with respect to the fitted potental constants V_3, V_6, V_{3c}', V_{3c}'' (Table 7).

$\overline{\partial\Delta\nu/\partial V_3}$	= $9.3\cdot10^{-3}$	MHz/GHz
$\overline{\partial\Delta\nu/\partial V_6}$	= $3.1\cdot10^{-3}$	MHz/GHz
$\overline{\partial\Delta\nu/\partial V_{3c}'}$	= $4.2\cdot10^{-4}$	MHz/(GHz·rad^{-1})
$\overline{\partial\Delta\nu/\partial V_{3c}''}$	= $2.2\cdot10^{-4}$	MHz/(GHz·rad^{-2})

[a] Defined as: $\frac{1}{N}\sum_{N}^{i}\left|\frac{\partial\Delta\nu_i}{\partial x}\right|$, for N splittings ($\Delta\nu_i$) and $x=V_3, V_6, V_{3c}', V_{3c}''$.

Table 11. Results obtained from the analysis of molecules presenting a RTV interaction and up to now studied in this laboratory. The zero values of some quantities are assumed.

		CH_3SCN [a]	CH_3CH_2CN [a]	CH_3SSCD_3 [b]	CH_3COCN [c]
V_3	GHz	16964	33824	15400	12346
V_6	GHz	0	−1805	0	−142
V_{3c}'	GHz·rad^{-1}	−5923	−14900	−1185	2649
V_{3c}''	GHz·rad^{-2}	0	0	0	5952
k_{2q}	GHz·rad^{-2}	450493	586274	216871	168948
k_{3q}	GHz·rad^{-3}	0	0	0	0
k_{4q}	GHz·rad^{-4}	0	0	0	0

[a] Reference [1]. [b] Reference [3]. [c] Present work.

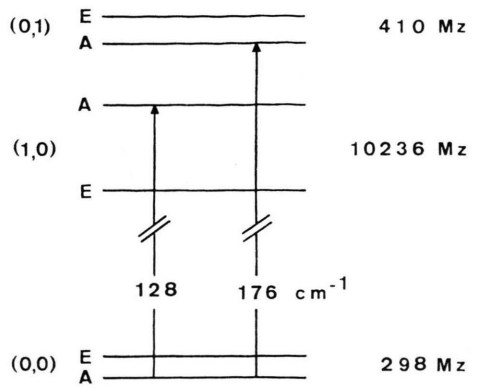

Fig. 3. Vibrational level scheme for CH_3COCN calculated with Hamiltonian (1) and the constants of Tables 5 and 7. The measured value for the v_α, v_q=0,0−0,1 transition is 176.0±0.5 cm^{-1} from gas phase infrared spectra, see Part III.

IV. Discussion

In acetyl cyanide the energy difference between the two interacting torsional and vibrational levels is about 50 cm^{-1}, and it is the largest within the series reported in Reference [1]. The satisfactory agreement between observed and calculated A-E rotational splittings (s. d. = 0.48 MHz or 2.8%) indicates that the RTV model used in this analysis is a far better approximation than the RFRT model. It must be pointed out that, while the A-E rotational splittings are correctly predicted, the frequencies of the corresponding transitions are not. This seems to be a general problem since all the analyses conducted with this kind of RTV model led to similar results [1, 3]. As Mäder et al. have discussed in the case of ethyl cyanide, there are reasons to believe that for a fit of both rotational constants and rotational splittings the RTV model has to be ultimately extended by consideration of other vibrations. Or, alternatively, the kinetic coefficients in (1) should be included, together with the potential parameters, in the fitting procedure.

Possible inaccuracies in the numerical treatment were eliminated or reduced to a reasonable extent troughout the calculations. The number of basis functions in the different steps of the diagonalization procedure was established by successive truncations of the matrices. An accuracy to 10 kHz in the calculation of the A-E rotational splittings was taken to be sufficient. In the present case it turns out that the following numbers of functions have to be taken into account: $17\,U_m(\alpha)$, $6\,U_{v_\alpha\sigma}(\alpha)$, $5\,H_{v_q}(q)$, and $18\,\Phi_{v_\alpha\sigma v_q}(\alpha, q)$. It has been numerically tested that the second order terms in the kinetic coefficients expressions do not affect the rotational splittings more than 1%. It seems therefore sufficient to consider terms up to the second order.

In the course of preliminary calculations to define the most suitable starting set of potential constants for the final least squares fit we observed that the calculated A-E rotational splittings and vibrational frequencies were rather insensitive to the sign of V_{3c}'. In fact with the same values of Table 7 but with a correspondingly negative value for V_{3c}' the A-E rotational splittings are still reasonably reproduced (s. d. = 0.75 MHz or 4.4%) while the vibrational frequencies are almost unaffected. This result is specifically connected with the numerical quantities which enter in the calculations for a particular molecule and has not to be generalized. It can be seen, looking at the matrix elements of the Hamiltonian (1) containing V_{3c}', that not only their signs are changed by reversing the sign of V_{3c}' but also their absolute values due to contributions from other parts of the Hamiltonian. The extent of this change is determined by the molecular quantities such as those of Table 5. Accordingly the sign of V_{3c}' may or may not be well defined.

A last comment refers to the quadrupole hyperfine structure. As in the ground state, even in the excited states (1, 0) and (0, 1) there are cases in

which slight discrepancies between A and E multiplets exist. These discrepancies mainly arise from inaccuracies in the measurements due to spectral complexity. They finally contribute to the errors by which the measured A-E rotational splittings are affected.

The restriction of our analysis to rotational transitions up to $J=5$ was only imposed by computer limitations. For one set of potential constants the evaluation of the rotational frequencies up to $J=5$ needs 51 kbytes and about 16 minutes central processor unit time with a PDP 10 computer, using double word precision to 16 digits [18]. A Van Vleck transformation of second order aimed at each $(1,0)$-, $(0,1)$-block separately prooved not to be sufficient in the case of acetyl cyanide [19]. This indicates that the two blocks should be treated together in the perturbation treatment.

The present investigation, including Part I, has shown that vibrational interactions, while not affecting the rotational spectrum of the ground state, do affect the spectra of the two next excited states. It seems likely that these interactions extend also to the first excited CCN-out-of-plane bending state observed at 245 cm^{-1}, see Part III. This state results to be close to the $(2,0)$-methyl torsion state calculated at 237 cm^{-1}. Further analysis of the rotational spectrum in the CCN-out-of-plane bending state would be extremely interesting in this respect and might also provide the experimental material for a more sophisticated RTV model with three internal degrees of freedom.

Acknowledgements

The authors want to thank Dr. H. M. Heise for discussions. The research funds and the research grant (F. S.) of the Deutsche Forschungsgemeinschaft and of the Fonds der Chemie are acknowledged. Calculations were carried out at the Rechenzentrum der Universität Kiel.

[1] a) References (2–6) of Part I. — b) H. M. Heise, H. Mäder, and H. Dreizler, Z. Naturforsch. **31 a**, 1242 [1976].
[2] Part I: F. Scappini and H. Dreizler, Z. Naturforsch. **31 a**, 840 [1976].
[3] M. Kuhler, L. Charpentier, D. Sutter, and H. Dreizler, Z. Naturforsch. **29 a**, 1335 [1974].
[4] T. Ikeda, R. F. Curl, and H. Karlsson, J. Mol. Spectrosc. **53**, 101 [1974].
[5] H. Karlsson, J. Mol. Struct. in press.
[6] S. S. Butcher and E. B. Wilson, J. Chem. Phys. **40**, 1671 [1964].
[7] E. Saegebarth and L. C. Krisher, J. Chem. Phys. **52**, 3555 [1970].
[8] M. Hayashi and K. Kuwada, J. Mol. Struct. **28**, 147 [1975].
[9] K. M. Marstokk and H. Møllendal, J. Mol. Struct. in press.
[10] B. Kirtman, J. Chem. Phys. **37**, 2516 [1962].
[11] C. R. Quade, J. Chem. Phys. **44**, 2512 [1966].
[12] J. V. Knopp and C. R. Quade, J. Chem. Phys. **53**, 1 [1970].
[13] A. Bauder and Hs. H. Günthard, J. Mol. Spectrosc. **60**, 290 [1976].
[14] H. Dreizler, Z. Naturforsch. **23 a**, 1077 [1968].
[15] H. Mäder, U. Andresen, and H. Dreizler, Z. Naturforsch. **28 a**, 1163 [1973]. Erratum: in Eq. (**41**) M^0 should be replaced by (1/2) M^0 and (1/2) V''_{3c} should be replaced by V''_{3c}.
[16] Part III: H. M. Heise, F. Scappini, and H. Dreizler, Z. Naturforsch. **31 a**, 1408 [1976].
[17] L. C. Krisher and E. B. Wilson, J. Chem. Phys. **31**, 882 [1959]. Erratum: **33**, 304 [1960].
[18] Computing programs: MRTVD1.F4 and MRTVD4.F4 by H. Mäder.
[19] Computing programs: DS1RTV.F4 and DS2RTV.F4 by U. Andresen.
[20] W. Gordy and R. L. Cook, Microwave Molecular Spectra, Interscience Publishers, New York 1970.